



Full Text View

[Volume 32, Issue 1 \(January 2002\)](#)

Journal of Physical Oceanography

 Article: pp. 55–79 | [Abstract](#) | [PDF \(682K\)](#)

Dynamics and Evolution of a Northern Meddy

Jérôme Paillet

Centre Militaire d'Océanographie, Service Hydrographique et Océanographique de la Marine, Brest, France

Bernard Le Cann

Laboratoire de Physique des Océans, Unité mixte CNRS-IFREMER-Université, Brest, France

Xavier Carton

Centre Militaire d'Océanographie, Service Hydrographique et Océanographique de la Marine, and Laboratoire de Physique des Océans, Unité mixte CNRS-IFREMER-Université, Brest, France

Yves Morel and Alain Serpette

Centre Militaire d'Océanographie, Service Hydrographique et Océanographique de la Marine, Brest, France

(Manuscript received December 7, 2000, in final form May 29, 2001)

DOI: 10.1175/1520-0485(2002)032<0055:DAEOAN>2.0.CO;2

ABSTRACT

A meddy was discovered in April 1997 off the northwestern corner of Spain, near 45°N, 11°30'W. It was tracked during 18 months with Lagrangian floats and deep drogued buoys, and several cruises were set to collect further hydrological and Lowered-ADCP measurements on it. The meddy, named Ulla, was a one-core lens with maximum values of temperature and salinity of 11.5°C and 36.17 psu near 1000-m depth, yielding anomalies above 2.5°C and 0.5 psu compared to its environment. Its rotation frequency was close to 1 loop every 5 days. The maximum azimuthal velocities of 15–20 cm s⁻¹ were reached near a 15-km radius. The meddy had a wide remote influence, notably up to the surface, and was associated with a total azimuthal volume transport of around 10 Sv, (Sv = 10⁶ m³ s⁻¹), of which around 2 Sv was trapped in the core. A widening of the radial structure with decreasing depth was notable in August 1997. Meddy Ulla was significantly elliptic for most of the time and, depending on the periods, the main ellipse axis either slowly rotated clockwise, or kept a constant orientation. The hydrological properties and vorticity of the core remained relatively constant during the observation period. Beyond the radius of maximum azimuthal velocity, the velocity structure was extremely variable and

Table of Contents:

- [Introduction](#)
- [Data](#)
- [Hydrological properties](#)
- [Dynamics of Meddy Ulla](#)
- [Time evolution of Meddy](#)
- [Summary and discussion](#)
- [REFERENCES](#)
- [TABLES](#)
- [FIGURES](#)

Options:

- [Create Reference](#)
- [Email this Article](#)
- [Add to MyArchive](#)
- [Search AMS Glossary](#)

Search CrossRef for:


- [Articles Citing This Article](#)

cannot be modeled simply. Meddy Ulla had two other characteristics that make it a particular member of the meddy family: first, it is the northernmost meddy, by around 5 latitude, that has ever been thoroughly studied. It is believed that Ulla was generated in the Cape Finisterre–Cape Ortegal area, far to the north of previously known formation sites. Second, Meddy Ulla stayed in the same area for 11 months while meddies usually drift quite rapidly, in a generally southwestward direction. Among the reasons advocated for its near stagnation are the frequent interaction with other “northern meddies” that drifted past Ulla to its south and the likely interaction with deep seamounts. After 11 months of stagnation, the meddy suddenly accelerated southwestward and lost some volume at the same time. Finally, after 18 months of observations, it was lost: at that time its net displacement was only 190 km southwestward, at a mean velocity of 4 mm s^{-1} . Meddy Ulla is the first of a series of “northern meddies” identified during the Action de Recherche sur la Circulation en Atlantique Nord Est (ARCANE) program.

Search Google Scholar for:



- [Jérôme Paillet](#)
- [Bernard Le Cann](#)
- [Xavier Carton](#)
- [Yves Morel](#)
- [Alain Serpette](#)

1. Introduction

Meddies are anticyclonic, subsurface vortex lenses full of warm and salty water of Mediterranean origin. They are prominent features of the North Atlantic hydrology, and have stimulated scientific interest for more than two decades. Nearly all meddies have been found east of the Mid-Atlantic Ridge in the Iberian and Canary Basins ([Armi and Zenk 1984](#); [Richardson et al. 1989, 1991](#); [Käse and Zenk 1996](#); [Richardson et al. 2000](#)). [Figure 1](#) , adapted from [Richardson and Tychensky \(1998\)](#) shows the distribution of meddies detected in historical data of the eastern North Atlantic. The meddy described in this paper, which was given the name Ulla (a Northern European name), was observed in 1997 and 1998 offshore of the northwestern corner of Spain, which is far to the northeast of the historical meddy distribution area. [Paillet et al. \(1999\)](#) showed near real-time tracking of that meddy for a year, and presented early results on its structure and dynamics.

The hydrological and dynamical properties of several meddies south of 40°N have been thoroughly described ([Armi et al. 1989](#); [Richardson et al. 1989](#); [Schultz Tokos and Rossby 1991](#); [Pingree and Le Cann 1993a,b](#); [Prater and Sanford 1994](#); [Tychensky and Carton 1998](#)). From these studies we learned that meddies are roughly circular lenses with thermohaline anomalies of typical diameter 30–100 km and thickness 500–1000 m, centered around a depth of 1000 m. Away from the Iberian Peninsula, maximum anomalies of temperature and salinity relative to their environment can reach 5°C and 1 psu. Meddies have a steep boundary in hydrological properties located at a radius of 10–40 km, thus defining the “core” and the “outside” of the lens. Within the core, the velocity distribution is close to a solid body rotation, and maximum azimuthal velocities are reached at radii slightly smaller than that of the steepest hydrological front. The outside region is characterized by a sharp decrease of azimuthal velocities and by thermohaline intrusions and hydrological inversions resulting from mixing, whereas the core is smooth and stably stratified. Vertical displacements of isopycnals tend to be larger below the core than above, and there is evidence that meddies can have a signature extending up to the sea surface ([Stammer et al. 1991](#); [Schultz Tokos et al. 1994](#); [Tychensky and Carton 1998](#)). Meddies occasionally exhibit a “double core” vertical structure, with two maxima in temperature and salinity anomalies, around depths of 800 and 1200 m, reminiscent of the double core structure of the Mediterranean outflow on the slopes of the Gulf of Cadiz.

The mechanisms for meddy formation have also been well discussed in recent literature. While a formation within the deep ocean has been proposed ([Käse and Zenk 1987](#)), it is now clear that the generation of most meddies takes place close to, or upon, the Iberian continental slope. In the Gulf of Cadiz and West Portugal regions the main veins of Mediterranean Water (MW), issued from the outflow at the Strait of Gibraltar, generally tend to follow isobaths poleward ([Madelain 1970](#); [Zenk 1975](#); [Ambar and Howe 1979](#); [Danialt et al. 1994](#); [Käse and Zenk 1996](#)), and many meddies have been shown to have the same hydrological properties as portions of MW veins on the continental slope (e.g., [Armi et al. 1989](#); [Pingree and Le Cann 1993a,b](#); [Prater and Sanford 1994](#)). Lagrangian floats have shown events of meddy formation and detachment from those veins ([Bower et al. 1995, 1997](#); [Chérubin et al. 2000](#); [Serra et al. 2001](#)). Several physical mechanisms of meddy formation have been propounded. Convective mixing followed by geostrophic adjustment, as proposed by [McWilliams \(1985\)](#), is probably not the major process because meddies seem to form significantly downstream, and not within, the area of MW sinking into the Atlantic. [D'Asaro \(1988\)](#) proposed a mechanism in which friction against the slope is the source for the anticyclonic vorticity of the eddy. [Bower et al. \(1997\)](#) acknowledge the likeliness of the latter process in the case of the meddies that they observe. [Pichevin and Nof \(1996\)](#) demonstrate that a zonal flow that rounds a cape to its right, such as the MW at Cape St. Vincent, is an unbalanced system and show that eddy generation can close this balance problem. Finally, the potential role of baroclinic instability has been demonstrated numerically by several authors, notably in the case of a poleward jet by [Käse et al. \(1989\)](#) and [Jungclauss \(1999\)](#). The likely influence of a deep canyon transverse to the MW flow (such as the Portimão Canyon along $\sim 8^\circ 32'\text{W}$) in triggering its baroclinic instability was also demonstrated numerically by [Jungclauss \(1999\)](#) and by [Chérubin et al. \(1996\)](#).



Using Lagrangian floats, [Bower et al. \(1997\)](#) identified two major meddy formation sites, Cape St. Vincent and the Estremadura Promontory¹ (see [Fig. 1](#) ). After their formation, meddies usually drift northwestward for a short period of time, after which nearly all meddies drift southwestward on average ([Richardson et al. 2000](#)). Thus, if all meddies were formed at the two above sites, it would be unlikely to find any to the north of 40°N. Indeed, all meddies that have been carefully sampled and studied before 1997 were found south of that latitude, the northernmost one, to our knowledge, being detected by [Hinrichsen et al. \(1993\)](#) near 40°N, 13°W. However, [Richardson et al. \(1991\)](#) and [Shapiro and Meschanov \(1996\)](#), searching for possible meddies in historical hydrographic data, detected five individual stations north of 42°N for which salinity near 1000-m depth exceeded the local climatology by more than 0.4, psu which Richardson et al. consider to be large enough to be representative of meddies. In [Fig. 1](#)  it is seen that the distribution of these anomalies is somewhat disjoint from the main, southern group of meddies, suggesting that a northern meddy source may exist.

In April 1997 a lens-shaped mesoscale structure was found during an Action de Recherche sur la Circulation en Atlantique Nord Est (ARCANE) cruise near 45°N, 11°30'W with high temperature and salinity near 1000-m depth, and happened to be a long-lived coherent vortex. In other words it was a meddy. [Paillet et al. \(1999\)](#) described its basic properties and early stages of evolution. The purpose of this paper is to analyze thoroughly the dynamics and time evolution of that meddy, using a more complete dataset. Another study currently under way, using hydrological measurements, current meter data, and Lagrangian trajectories collected during the ARCANE program, will show that “northern meddies” (i.e., north of 40°N) are indeed common features.

The paper is organized as follows: The dataset is described in [section 2](#). The hydrological and dynamical properties of the meddy are discussed in [sections 3 and 4](#). [Section 5](#) describes the meddy trajectory and several aspects of its time evolution. Finally, the main findings are summarized and discussed in [section 6](#).

2. Data

a. One year of measurements and float deployments

The ARCANE program ([Le Cann et al. 1999](#)) is a collaboration between Laboratoire de Physique des Océans, France, Service Hydrographique et Océanographique de la Marine, France (SHOM), Instituto Hidrografico, Portugal, and Woods Hole Oceanographic Institution to study the circulation in the eastern North Atlantic midlatitudes, with a particular focus on processes near the Iberian continental slope. Ships were at sea several times a year from 1996 to 1999 for that program, in order to deploy floats, to maintain a current meter array and to collect hydrological measurements. In April 1997 a meddy was discovered from aboard BO *D'Entrecasteaux* at a surprisingly northerly position (45°N, 11°30'W), and was named “Ulla.” Horizontal maps of temperature at 1000 and 1200 m, drawn from those measurements, are shown in [Fig. 2](#) . They reveal unambiguously the presence of the meddy, with a temperature anomaly relative to its environment of more than 2°C at 1200-m depth. Meddy Ulla was tracked in near real time (see [Paillet et al. 1999](#)) using deep-drogued Surdrift buoys and in delayed time using RAFOS and Marvor floats (described thereafter), which allowed us to return to it several times in 1997–98. [Table 1](#)  lists the cruises that collected measurements and seeded floats in Meddy Ulla. Those cruises were not primarily devoted to collect measurements in the meddy, hence most observations were done quickly with expendable probes and few CTD casts. The most precise and complete measurements were gathered during the NO *Thalassa* cruise of August 1997. Those measurements will be extensively discussed herein. By March 1998, no Surdrift remained close enough to the meddy center to accurately locate it, and most information was provided in delayed time by Marvor floats. Therefore, unfortunately, the meddy center could not be found during the cruises of March and April 1998 and the last Surdrifts, released near the edge of the core, were not trapped in the meddy. We thus lack a good hydrological description of Ulla after August 1997, which could have helped us determine how much it decayed.

b. Lagrangian trajectories

Three types of floats and drifters were released in Meddy Ulla:

- The Surdrift buoy is a deep-drogued buoy developed by SHOM. It consists of a small surface buoy positioned by the Argos satellite system, a near-surface elastic shock absorber, a thin (2.1 or 3 mm diameter) Kevlar cable, and large (10 m² vertical cross section) cylindrical holeysock drogue. The drogue is constrained to remain vertical by buoyancy above and ballast below. Surdrifts are not really Lagrangian, as their displacement is influenced by currents at all depths between the surface and their drogue depth. However several experiments of SHOM since 1995, with drogues as deep as 1300 m, showed they could efficiently follow a meddy, or a MW vein ([Chérubin et al. 2000](#)). A Surdrift with a cable 1000 m long and a pressure gauge at the drogue level was once deployed for a few days in a meddy: the drogue remained between 950 and 1000 dbar, which shows that the cable remained nearly vertical even in relatively strong velocity shear conditions.
- The Marvor is a multicycle, isobaric, acoustic subsurface float. It is positioned from moored sound sources by

listening and recording the times of arrival (“RAFOS” technology). It looks for a prescribed pressure level by activating an external bladder. After drifting a prescribed time at that level, it surfaces to transmit the cycle data, before diving for the next cycle.

- Classical RAFOS floats were also deployed. They are preballasted to a target pressure level, and complete only one subsurface cycle before dropping a weight, surfacing, and transmitting all the data.

The positions of acoustic sources used for tracking Marvor and RAFOS in the area are shown in [Fig. 1](#). Floats listened to these sources one or three times a day and recorded the ambient pressure and temperature with the same frequency. A gross estimate of the acoustic positioning error, based on the distance between the first ARGOS surface fix and the last underwater acoustic positioning, is about 5 km for the absolute positioning (the relative error within a trajectory being likely much smaller). [Table 2](#) summarizes information on all ARCANE drifting instruments, either successfully deployed in Meddy Ulla, or deployed elsewhere but happening to fall within its influence for a significant time. A total of 18 floats and drifters operating from 150 to 2000 m depth were involved, which is an unprecedented Lagrangian dataset for a single eddy—even though a majority of those floats spent only a minor part of their life within Meddy Ulla. Two Rafos and one Marvor float completed more than 60 loops in the meddy.

[Figure 3](#) displays trajectories of a selection of floats and Surdrifts that felt Meddy Ulla's influence. Those trajectories were low-pass filtered to remove high frequency motions (periods < 1 day) and noise. As the meddy remained nearly stationary for 11 months, the period is divided into distinct time phases, in order to get interpretable figures:

- *Phase 1, 15 April–15 August 1997:* [Figures 3a,b](#) show five trajectories during that first 4-month period. Two deep-drogued Surdrift (1100 and 1200 m) remained within Ulla for the entire period ([Fig. 3a](#)), This is remarkable for such deeply drogued drifters. RAFOS 634 near 1200-m depth also remained within the meddy core ([Fig. 3b](#)), while RAFOS 639, launched at the same time and location, but ballasted deeper (1440 dbar), left it after three loops. Marvor 404 at 1000 dbar, released earlier and outside the meddy, happened to complete one loop around it at a radius of around 50 km, during the same phase. During these 4 months Meddy Ulla first drifted northwestward, then southwestward, westward and back eastward.
- *Phase 2, 15 August–15 December 1997:* On 15 and 16 August, floats were released at several levels in the meddy ([Table 1](#)). [Figures 3c,d](#) show the tracks of five of those floats, together with the continuation of the Rafos 634 track. Marvor 656 at 1000 dbar was programmed to cycle frequently (30 days) and completed four cycles during phase 2 without leaving the meddy. Surdrift 494 at 150 dbar ([Fig. 3c](#)) and Marvor 8124 at 450 dbar ([Fig. 3d](#)) completed 2 and 3 loops, respectively, before leaving the meddy. Marvor 8123 at 1500 dbar completed four loops during its first 3-month cycle, and moved from the meddy center, before leaving the meddy during its second cycle (not shown for clarity). Finally, Marvor 8122 at 2000 dbar ([Fig. 3c](#)) hardly felt Ulla's influence: after completing about one-quarter loop, it drifted northeastward and slowly away from the meddy center. These trajectories indicate that, while rotating under the meddy's influence, fluid parcels above 450 dbar and below 1500 dbar were not “trapped” in it. During phase 2 Meddy Ulla completed a small clockwise loop that ended around 45°N, 11°40'W, quite close to where it was first discovered.
- *Phase 3, 15 December 1997–15 March 1998:* We isolate this 3-month phase for clarity, as the meddy's behavior changed abruptly after that phase. In early December, Surdrift 509, anchored at 1000 m, was released about 8 km from the meddy center. [Figure 3e](#) shows that it remained within the meddy during phase 3 but ended up some 30 km away from the center. At the same time Marvor 656 completed three more 30-day cycles within Ulla. During phase 3 the meddy slightly drifted northward, reaching its northernmost latitude of 45°30'N in the first half of March 1998.
- *Phase 4, 15 March–18 October 1998:* Meddy Ulla suddenly started drifting southwestward at the beginning of this period. This is revealed in [Fig. 3f](#) by two floats that were not shown before: Marvor 657 was released at 1000 dbar in August 1997, and had a long underwater cycle of 7 months ([Table 2](#)). This was aimed at giving it more chances to remain within the meddy for a long time. That goal was reached, as its entire second cycle, until 18 October 1998, took place within the meddy. Unfortunately, due to a technical problem there are gaps in its acoustic positioning, which make the track less precise than that of other floats. RAFOS 635, drifting around 1220 dbar, was released in June 1997 for 1 yr. In the first 10 months it behaved very similarly to RAFOS 634 displayed in [Figs. 3b,d](#), and remained two more months underwater after the latter float surfaced in April 1997. During the last 3 months of its trajectory, displayed in [Fig. 3f](#), it followed Ulla in its southwestward drift until approximately 14°W, after which it left the meddy and moved due westward. [Paillet et al. \(1999\)](#) show how Marvor 656 at 1000 dbar similarly left the meddy in its southwestward drift, around 13°W. Surdrift 509 shown in [Fig. 3e](#), and Surdrift 496 released in March 1998 also failed to follow the meddy during that phase. This suggests that the meddy's acceleration was accompanied by some significant loss of particles. Another ARCANE RAFOS, number 651 near 1140 dbar, found itself on the meddy's southwestward path ([Fig. 3f](#)): it was entrained in a large anticyclonic loop some 50 km from the meddy center, before surfacing for the end of its mission.

A detailed analysis of the meddy dynamics and behavior will be presented in [sections 4 and 5](#). In [section 3](#), we first describe its hydrological properties.

3. Hydrological properties

a. Temperature and salinity

The tracking of Meddy Ulla with Surdrifts 834 and 836 ([Fig. 3a](#)), and later with Surdrifts 493 and 509, allowed us to estimate the meddy center position in slightly delayed time, and to guide ARCANE cruises toward it. The most precise and complete measurements were done in August 1997 aboard NO *Thalassa* ([Table 1](#)). During four days, a large crosslike array of 26 stations was completed ([Fig. 4](#)). At each station, CTD, Lowered-ADCP acoustic Doppler current profiler data and water samples were collected down to 3000 dbar or the ocean bottom. Also shown in [Fig. 4](#) is the track of RAFOS 634 at the time of those measurements: it provides an independent confirmation that the center of the cross was very close to the meddy center. [Figure 5](#) shows potential temperature and salinity sections along the meridional and zonal lines of the cross. Meddy Ulla appears as a classical, lens-shaped structure centered around 1000-m depth. If we define the 11°C isotherm or the 36.0 isohaline as its hydrological boundary, its apparent diameter is ~ 60 km along the zonal line and only ~ 45 km along the meridional line. This is not due to a sampling problem, as the center of the cross coincides well with the meddy center, which moved little during those 4 days. It is due to the meddy ellipticity, also shown by the RAFOS 634 trajectory on [Fig. 4](#). The question of ellipticity will be dealt with in detail in [section 5](#). Ulla was a medium size meddy, larger than [Prater and Sandford's \(1994\)](#) lens of ~ 30 km diameter in the Gulf of Cadiz, and smaller than [Tychensky and Carton's \(1998\)](#) Meddies Hyperion and Encelade of ~ 90-km diameter southeast of the Azores.

Unlike some meddies found more to the south (e.g., [Richardson et al. 1989](#); [Prater and Sandford 1994](#); [Arhan et al. 1994](#)), Meddy Ulla had only one core of temperature and salinity. Maximum potential temperature, ~ 11.4°C (in situ temperature ~ 11.5°C), was found between 850 m and 900 m depth. Maximum salinity, ~ 36.17 psu, was found between 1020 m and 1080 m depth. The one-core structure, with a vertical shift between T and S maxima, is similar to that of the MW vein north of 40°N. There was small-scale temperature and salinity variability on the edge and outside of the meddy, while its inner core (stations 35–37 and 47–49) was devoid of such structures from 800 m to 1200 m depth. The presence of finestructure on the meddy lateral boundaries, also illustrated for other meddies by [Ruddick and Hebert \(1988\)](#), [Armi et al. \(1989\)](#), or [Pingree and Le Cann \(1993a\)](#), most likely reflects mixing by lateral intrusions.

b. Thermohaline anomalies

[Figure 6](#) displays the anomalies, relative to the four outer stations of the cross, of θ , S , and σ_1 (potential density relative to 1000 dbar) along the *Thalassa* 97 meridional line. Such a representation shows how the meddy differs from its neighboring environment, evidencing its signature more efficiently than the original parameters. The σ_1 section along the same line is shown in [Fig. 6d](#) for comparison purpose. [Figures 6a,b](#) show that the thermohaline signature of the meddy is significant only between 600 m and 1600 m depth, with a maximum anomaly around 1200 dbar for both θ and S . Those maximum anomalies are slightly greater than 2.5°C and 0.5 psu, respectively. Meddy Ulla satisfies the criterion used by [Richardson et al. \(1991\)](#) to detect meddies in historical data (i.e., $\Delta S > 0.4$ psu over a 200-m thickness).

A good indicator of the meddy's dynamical signature is its potential density anomaly, directly related, through the thermal wind balance, to the baroclinic velocity shear. The anomaly of σ_1 ([Fig. 6c](#)) shows two areas of opposite anomaly associated with the meddy: between 1600 and 950 dbar, the anomaly is significantly negative and corresponds to anticyclonic velocity shear (going upward); between 900 and 500 dbar, it is significantly positive and corresponds to cyclonic velocity shear. As frequently observed in other meddies, the σ_1 anomaly is not vertically symmetric, the negative pole being more intense than the positive one. This ensures, provided that the deep flow is vanishing, that the structure is anticyclonic everywhere and has a near-surface dynamic signature. The negative σ_1 anomaly extends down to 2500 dbar, consistently with a deep anticyclonic signature of the meddy. However, below 1600-m depth the anomaly is not due to warm and salty MW but to relatively cold and fresh water ([Figs. 5 and 6a,b](#)) that, in this depth range, is Labrador Sea Water (LSW). During the initial *D'Entrecasteaux* cruise in April 1997, there was no such patch of LSW right below the meddy, but there was one slightly to the west [see [Fig. 1](#) of [Paillet et al. \(1999\)](#)]. In June 1997 a patch of LSW was also detected, to the north of the meddy. The meddy had perhaps aligned vertically with that, or with another, anticyclonic patch of LSW between June and August.

Other features of interest are the negative patches of σ_1 anomaly to the north and south of the meddy, in the range (0, 900 m) and (0, 400 m), respectively. Another such feature exists to the east of the meddy (see the upper isotherms and isohalines in [Fig. 5](#) right). This may be associated with small, surface-intensified anticyclonic eddies, or to a larger scale anticyclonic flow above the meddy. The dynamical signature of these features will be discussed in the next section.

4. Dynamics of Meddy Ulla

a. Direct measurements of velocity

During the *Thalassa 97* cruise, each CTD cast was achieved with a Lowered-ADCP (LADCP) current meter fixed on the rosette. Velocity profiles were obtained through vertical integration of the measured velocity shears over the duration of a cast and correction of the barotropic component for the ship drift, as described by [Fischer and Visbeck \(1993\)](#). [Figures 7a,b](#) show the distribution of the LADCP velocity component normal to both lines of the measurement array ([Fig. 4](#)).

CTD data were used to compute cyclogeostrophic velocities relative to 3000 m across those lines, by a vertical integration of the gradient wind balance in cylindrical coordinates (assuming a circular symmetry):

$$\left(f + 2\frac{u_\theta}{r}\right)\left(\frac{\partial u_\theta}{\partial z}\right) = \frac{-g}{\rho_0} \frac{\partial \rho}{\partial r},$$

where u_θ is the azimuthal velocity, r the distance to the meddy center (at 45.05°N, 12.30°W in the present case), f the Coriolis parameter, g the gravitational acceleration, ρ density, and ρ_0 a reference density. Here the cross-section velocity is considered as an azimuthal velocity, because the meddy center lies very close to the line axis. [Figures 7c,d](#) present those velocities across the same two lines (estimated at midpoints between station pairs).

First one should note the good overall agreement between direct LADCP measurements and cyclogeostrophic estimates. This agreement is not straightforward because the LADCP also measures the high frequency component of velocity and is contaminated by noise, while the cyclogeostrophic estimate may be biased by the internal wave field, the choice of a reference level, and the noncylindric symmetry of the meddy. Geostrophic velocities were also computed (without the centrifugal correction in the above equation). As expected, they are in less good agreement with LADCP measurements, the maximum geostrophic velocities being less intense than the cyclogeostrophic ones by typically 20%.

Meddy Ulla stands out as the main signal in [Fig. 7](#), with a quasi-symmetric velocity pattern centered on station pairs 35–36 ([Figs. 7a,c](#)) and 47–48 ([Figs. 7b,d](#)). Maximum velocities between 15 and 20 cm s⁻¹ are observed near 900–1000 m depth, within 15–25 km from the meddy center. Velocities above 10 cm s⁻¹ are observed from 1300 to 1500 m to around 600-m depth in most cases. The meddy's influence up to the surface is obvious. This has been observed for several meddies in the past (e.g., [Stammer et al. 1991](#); [Schultz Tokos et al. 1994](#); [Tychensky and Carton 1998](#)).

What is original in the present case is the evidence that the radial structure of velocity widens with decreasing depth (clearly in [Figs. 7a–c](#), but not in [Fig. 7d](#)), maximum azimuthal velocities near the surface being found further away (25–30 km) from the meddy center than at the core level. One hypothesis for this phenomenon is the following: when a meddy moves into a fluid initially at rest, it compresses fluid columns above and below. Through potential vorticity conservation, anticyclonic relative vorticity is generated to compensate vortex stretching. This accounts for the general anticyclonic circulation found all around the meddy. The baroclinic adjustment of the upper layer across the main pycnocline must occur on the scale of the first baroclinic radius of deformation,² which is larger than the meddy scale itself. The wider scale of anticyclonic circulation near the surface is consistent with the areas of negative density anomaly found above and at the periphery of the meddy, shown in [section 3](#) above. Azimuthal velocities east of the meddy also suggest the presence of a distinct southward jet that could be the signature of a surface anticyclonic eddy advected along to the south of the meddy. This could partly explain why the meddy widening is not apparent in [Fig. 7d](#).

Larger velocities are observed across the meridional line as could be expected from the elliptic shape of the meddy, elongated in the zonal direction (see [section 3a](#)). The total azimuthal volume transports, integrated from 100 m to 3000 m depth and from the meddy center to the outermost CTD–LADCP stations, amount to around 10 Sv (1 Sv ≡ 10⁶ m³ s⁻¹) for both sections and both velocity estimates, except across the western part of the zonal line (~5.5 Sv, but some of the associated northward transport may be found farther west). However, the volume transport of the anomalously salty water ($S > 35.8$) is only around 2 Sv: this illustrates how the dynamical influence of a meddy extends far beyond its radius of thermohaline influence.

b. Potential vorticity (PV) structure from hydrography

The vertical component of Ertel's potential vorticity,

$$q = (f + \zeta) \frac{1}{\rho_0} \frac{\partial \rho_p}{\partial z},$$

where ζ is relative vorticity and ρ_p potential density referred to local pressure, can be estimated from hydrography alone.

[Figure 8a](#) displays the distribution of planetary vorticity

$$\text{PV} \left(\frac{f}{\rho_0} \frac{\partial \rho_p}{\partial z} \right)$$

along the meridional line of the *Thalassa 97* dataset, and [Fig. 8b](#) the normalized relative vorticity ζ/f along the same line, estimated from the cyclogeostrophic velocity through




$$\zeta = \frac{u_\theta}{r} + \frac{\partial u_\theta}{\partial r}.$$

LADCP velocities were also used to estimate the relative vorticity, giving similar results. [Figures 8c](#) display the total Ertel PV, and [Fig. 8d](#) its anomaly relative to the outer stations of the line (calculated along iso- σ_1). The planetary and total PV distributions ([Figs. 8a,c](#)) are classical for a meddy: a tripolar structure on the vertical, with a pole of minimum stratification inside the haline core, and two poles of maximum stratification above and below, accounted for by the squeezing of isopycnals. The normalized relative vorticity ζ/f amounts to -0.25^3 within the meddy core, so that the total PV is close to $3.5 \times 10^{-11} \text{ m}^{-1} \text{ s}^{-1}$ in the core. This value is larger than those found within relatively young meddies found farther south like Bobby ($< 2 \times 10^{-11} \text{ m}^{-1} \text{ s}^{-1}$; [Pingree and Le Cann 1993a](#)) or Cadiz ($< 1 \times 10^{-11} \text{ m}^{-1} \text{ s}^{-1}$; [Prater and Sandford 1994](#)), and close to that obtained within the older meddy Sharon ([Schultz Tokos and Rossby 1991](#)). This does not imply that Meddy Ulla is old, as it is likely to have formed from a relatively weak MW vein, far from the strongest MW currents and lateral shears of the Gulf of Cadiz. For both lines, and using hydrography-derived velocities or LADCP data, relative vorticity changes sign about 30 km away from the meddy center. This change of sign is not sufficiently strong as to imply a similar change of sign in the total PV anomaly, shown in [Fig. 8d](#). This anomaly also exhibits the classical tripolar structure on the vertical. The lower positive pole is less marked than the upper one, and both are somewhat discontinuous, with distinct maxima between 25 and 50 km from the meddy center. Those maxima confirm that the meddy has a dynamical influence on the upper and lower layers, on a wider scale than its own structure. The separated negative pole in the near-surface layer above the meddy is partly an artifact of the relatively high PV values in this density range at station 42. Nevertheless, a stratification minimum and an oxygen maximum (not shown) do exist above the meddy core around 200-m depth.


c. Meddy dynamics from float trajectories

Float trajectories are filtered to isolate the movement of particles relative to the meddy center. The method should be insensitive to meddy shape and to radial movements of the floats. Therefore, Fourier-like filters, or fits to a cycloidal curve, are discarded. Instead, we choose to estimate the meddy center position by computing a running mean over exactly one rotation period of the float, evolving with time. [Figure 9](#) illustrates the results with the example of Rafos 634 trajectory ([Fig. 9a](#)). First, high-frequency motions and noise ($T < 1$ day) are low-pass filtered. Then the rotation period ([Fig. 9b](#)) is estimated iteratively: the trajectory is first high passed over a first guess window period; the heading of the relative trajectory goes to zero once a loop, which allows a second guess of the rotation period; the operation is repeated until convergence. The running mean over the (evolutionary) rotation period is an estimate of the meddy center trajectory ([Fig. 9a](#)). The trajectory relative to the moving center ([Fig. 9c](#)) looks reasonably smooth and centered on zero, showing the efficiency of the filter. [Figure 9d](#) shows the time evolution of distance between the float and the meddy center: its low frequency evolution is consistent with that of the rotation period (the farther the float from the center, the larger the rotation period), but that evolution is clearly perturbed by high frequency modes that appear to be dominant at half the meddy rotation period (mode two, due to ellipticity). Rotation frequency $\omega(r)$ ([Fig. 9e](#)) and azimuthal velocity $\mathbf{v}_\theta(r) = r\omega(r)$ ([Fig. 9f](#)) relative to the meddy center are estimated as averages over half a rotation period, to avoid pollution by ellipticity effects. The $\omega(r)$ distribution for RAFOS 634 is centered around $-1.5 \times 10^{-5} \text{ rad s}^{-1}$ (around 1 loop in 5 days) up to $r = 10$ km, and shows a slight decrease at greater radial distance. The $\mathbf{v}_\theta(r)$ relation is accordingly quasi-linear up to $r = 10$ km, and shows a tight distribution.



The same processing method was applied to all floats. For those floats that completed less than 5 loops (see [Table 2](#)), the meddy center position was not calculated from the trajectory itself but from a least squares fit of estimates from other


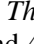
floats. [Figure 10](#)  shows the distribution of $\mathbf{v}_\theta(r)$, gathered from all Lagrangian floats located between 1000 m and 1200 m depth, except Marvor 657, which was too badly located. For radii greater than 20 km, data comes from floats M 404 ([Fig. 3b](#) ) , R 650 (not shown), and R 651 ([Fig. 3f](#) ) , which went looping around Ulla from the outside. These data are not corrected for ellipticity because of the very few loops in these trajectories and the quite varying radial distance from the meddy center. Instead, for these floats, averages of \mathbf{v}_θ and r are computed over 4-day time lags. LADCP data from *Thalassa 97*, averaged between 1000 m and 1200 m depth and corrected for ellipticity (assuming azimuthal transport conservation), are also plotted. Despite the different depths of the floats, and the time window of more than the $\mathbf{v}_\theta(r)$ relation is quite tight within the first 10 km from the center, and close to a linear relation typical of a solid body rotation. Maximum azimuthal velocities are in the 15–20 cm s⁻¹ range at $r \sim 15$ km. The $\mathbf{v}_\theta(r)$ relation is much more scattered beyond $r = 15$ km, even within each individual dataset (LADCP data or individual float data). This cannot be simply attributed to meddy ageing or to float depth differences, as some data from R651, both relatively deep (~ 1140 dbar) and relatively late (starting May 1998) indicate large azimuthal velocities at large r . The scatter mainly comes from the fact that the meddy was surrounded by other eddies and mesoscale motions, as will be illustrated in [section 5](#).

Estimates of the meddy core rotation frequency, computed individually from floats R634, R635, M 656, and M 657 and for different phases of the first year, agree within 15%, ranging from -1.37 to $-1.59 \times 10^{-5} \text{ s}^{-1}$. Absolute values of rotation frequency deduced from the deep-drogued Surdrift buoys are low by typically 20%–30%, showing that Surdrift data, while of great use to track the meddy, are improper for accurate dynamical calculations.


[Figure 10](#)  illustrates how hard it is to model the meddy's remote horizontal influence. Two models of the meddy radial structure at 1000–1200 m are nevertheless proposed, both corresponding to vortex types used in the literature. One is the Rankine vortex, $\mathbf{v}_\theta(r) = \omega_0 r$ for $0 < r < R_0$, and $\mathbf{v}_\theta(r) = \omega_0 R_0 / r$ for $r > R_0$ (where ω_0 is the rotation frequency at the center). It has a piecewise constant vorticity, equal to zero beyond the discontinuity radius R_0 . The other is a Rayleigh vortex,

$$\mathbf{v}_\theta(r) = \omega_0 r \times e^{-r^2/L^2}$$

(where L is the scale of radial decrease) corresponding to a Gaussian streamfunction, and also used in the literature to fit observed vortex velocity distributions (e.g., [Pingree and Le Cann 1993a,b](#)). Both models are least squares fitted to the data. They yield a proportionality relation at the origin, with slopes ω_0 of -1.42 and $1.50 \times 10^{-5} \text{ s}^{-1}$, respectively. These slopes show that the relative vorticity in the core ($2\omega_0$) is close to $-3 \times 10^{-5} \text{ s}^{-1}$ or $-0.3f$. Beyond $r = 15$ km, the Rankine ($1/r$ -like) fit values probably increase too sharply at medium radii and too gently at large radii, while the Rayleigh fit goes to zero for too small radii (~ 60 km). The relative vorticity $\zeta(r)$ associated with the Rayleigh fit is also shown in [Fig. 10](#) : from a value of $-3 \times 10^{-5} \text{ s}^{-1}$ at the center, it goes to zero near $r = 27$ km and is positive beyond, which is consistent with the observed distribution of ζ ([Fig. 8b](#) ).

The same data processing applied to floats at all depths allows the study of the meddy vertical structure. [Figure 11](#)  displays the rotation frequency ω , averaged from float trajectories in two radius ranges, (0–10 km) and (15–20 km), for six depth levels. The frequency ω is preferred to \mathbf{v}_θ in the present case because it is more constant with r . The figure confirms that the vertical structure is not fully symmetric, with generally larger velocities above than below the core. In particular, the meddy signature is quite stronger at the 150-m level than at the 2000-m level. The widening of the structure with decreasing depth, noted from the *Thalassa 97* data, also appears in [Fig. 11](#)  since ω decreases proportionally less, from (0–10 km) to (15–20 km), at 150 and 450 m than at 1000 and 1200 m. The same reasoning may also indicate a widening with *increasing* depth below 1200 m, although this is less conspicuous as the 2000-m values, notably, rely on little data.

d. Nondimensional numbers

We can derive nondimensional numbers from the available data ([Table 3](#) ) , to compare with observations of Meddies in a similar fashion to [Prater and Sanford \(1994\)](#). With their notations, we obtain a “velocity” Rossby number $R_\mathbf{v} \sim -0.24$ and a lengthscale Burger number $B_L \sim 0.5$. Compared to “historical meddies” values in their Fig. 19, Ulla's Rossby number is in the low range and its Burger number is in the high range. The former can probably be explained by the fact that Ulla was formed at a location where horizontal velocities (and Rossby numbers) of the MW undercurrent are lower than at the more southerly formation sites of these historical Meddies. The latter may be an indication that Ulla was relatively young, like two other meddies presenting a very large Burger number of $B_L \sim 1.4$, meddy “Cadiz” ([Prater and Sandford 1994](#)) and the “Smeddy” of [Pingree and Le Cann \(1993b\)](#). The Burger number of order 1 means that Ulla was stable and not prone to

either barotropic ($B_L \gg 1$) or baroclinic ($B_L \ll 1$) instability (McWilliams and Gent 1986).

5. Time evolution of Meddy Ulla

a. Meddy trajectory

The 18-month-long trajectory of Meddy Ulla is displayed in Fig. 12 within the bathymetric context. The different phases of movement were examined earlier in section 2. Figure 12 outlines how little the meddy moved from 15 April 1997 (day 1) to 11 March 1998 (day 330) when it reached its northernmost latitude of $45^{\circ}32'N$. The net movement over that 11-month period was about 40 km northward. Then, Ulla accelerated southwestward to reach its southernmost latitude of $42^{\circ}30'N$ on 28 August 1998 (day 500). Finally, Ulla returned northward to $44^{\circ}N$, after which it was no longer tracked. Over 550 days, the net movement was only 4 mm s^{-1} southwestward.

So far, all meddies tracked with floats for more than 3 months had net displacements between a southward and a westward direction, at mean velocities between 1 cm s^{-1} and 7 cm s^{-1} (Richardson et al. 2000). Some of them were observed to alternate periods of movement and stall like Ulla, but none stalled for more than 1 or 2 months.

Ulla was not really motionless during its period of stagnation. Figure 13 shows the time evolution of the meddy center velocity. The mean velocity modulus is 2.8 cm s^{-1} , and is typically $1\text{--}2 \text{ cm s}^{-1}$ during periods of stall, which is not very small: as obvious in Figs. 3 and 12, the meddy did move, but back and forth. A first southwestward acceleration occurred near day 50, but the meddy did not cross the Charcot Seamounts and returned eastward after day 80. The second acceleration, after day 300, was briefly eastward then southwestward, associated with translation velocities up to 10 cm s^{-1} . This brought the meddy back to where the first southwestward drift stopped, near the eastern flank of the Charcot Seamount. This time, the seamounts were crossed within a few days, and the following drift (southward until day 500 and back northward until day 550) remained associated with relatively large velocities of about 5 cm s^{-1} . Reasons for the absence of net southwestward drift during the first 11 months are now examined.

b. Why was Ulla so stationary?

In a fluid at rest, a meddy tends to drift southwestward under the influence of the planetary β effect at an average displacement speed of $1\text{--}2 \text{ cm s}^{-1}$ (McWilliams and Flierl 1979; Morel and McWilliams 1997). The following processes may result in a departure from that general behavior:

1. Interaction between meddy and topography
2. Interaction between meddy and large-scale circulation
3. Interaction between meddy and other mesoscale eddies.

The first process, interaction with topography, comes to mind immediately when looking at Fig. 12: the Charcot Seamounts seem to inhibit any southwestward translation of the meddy until day 360. The σ_3 vertical sections computed from CTD casts (not shown here—see the shape of the $\sigma_1 = 32.5$ isopycnal in Fig. 6d), clearly indicate that the depression of isopycnals associated with the meddy extended to depths of $\sim 3500 \text{ m}$, making direct interactions with the Charcot Seamounts possible. Numerical studies have indeed shown the possibility of vortex trapping by a seamount in a barotropic model (Van Geffen and Davies 2000). For baroclinic vortices with weak deep flows such as Meddy Ulla, theoretical and numerical results have shown that simple bottom topography can slow down the vortex propagation and trap the vortex for a while (see Thierry and Morel 1999, and references therein). However, to our knowledge, no studies lead to a stalling period as long as that observed for Meddy Ulla. This suggests that either the complex interaction with all the neighboring seamounts or another mechanism have to be taken into account to explain the long trapping of Ulla.

The second process, interaction with the wider-scale circulation, is hard to test as it would require a monitoring of that circulation. Vandermeirsch et al. (2001) results indicate that only the barotropic part of large-scale currents have a strong influence on vortex displacement, so that a significant northeastward mean transport is needed to oppose the planetary β effect. The inverse model of Paillet and Mercier (1997), based upon data from the 1980s in the eastern North Atlantic, does not show such a flow in that area, but instead a very weak southwestward circulation from the surface to 1000 m. Velocities measured in the vicinity of Ulla during ARCANE cruises, such as during *Thalassa 97* (Fig. 7), or tracks of other ARCANE floats that drifted in the vicinity of Ulla (Figs. 14–15), also do not show a firm northeastward trend. The area where Meddy Ulla was trapped is a region of quite weak mean flows dominated by relatively strong variability on

timescales of a few months (Gould 1983), and it is thus unlikely that a steady flow could have blocked Ulla for 11 months.

The third process, interaction with other mesoscale eddies, is likely to have occurred at least for some time, but only specific types of interaction may lead to the blocking of a meddy. One is the coupling with a neighboring cyclone (see, e.g., Hogg and Stommel 1985). Such a dipole may propagate northeastward, opposite to the propagation of a monopolar anticyclone, if the cyclonic vortex is located to the northwest of the anticyclone. There is, however, no evidence for a persistent cyclone in the northwest of Ulla, neither in hydrographic nor in float data (Figs. 14–15). Another possibility is interaction with other meddies. Figure 14 displays the trajectories of floats caught in four vortices that passed within the vicinity of Ulla. Three of them are meddies (or, at least, anticyclones in the 1000–1200 m depth range) that drifted southwestward on the southeastern side of Ulla. In such an anticyclone–anticyclone interaction, each vortex is expected to induce a displacement of the other, with a direction and magnitude similar to that of a fluid parcel at the same location if the vortex was alone. Thus, the three meddies that passed south of Ulla may have induced a generally eastward velocity on it. Meddy 1 is weaker than Ulla ($\mathbf{v}_\theta \sim 10 \text{ cm s}^{-1}$ at $r = 15 \text{ km}$, compare with Fig. 10) but comes quite close to it ($\sim 80 \text{ km}$). Meddy 2 and Meddy 3 are stronger than Ulla (M2: $\mathbf{v}_\theta \sim 20 \text{ cm s}^{-1}$ at $r = 28 \text{ km}$; M3: $\mathbf{v}_\theta \sim 20 \text{ cm s}^{-1}$ at $r = 10 \text{ km}$) and come to within 150 and 100 km from Ulla, respectively. At such distances, induced velocities of 1–3 cm s^{-1} are well plausible: with a Rankine velocity distribution, the above numbers imply velocities of 1.9 cm s^{-1} for M1, 3.7 cm s^{-1} for M2 and 2 cm s^{-1} for M3, at the distance of Ulla. Figure 14b also shows a cyclone, revealed by a RAFOS float near 520 dbar, that was born just before meddy 3 offshore Cape Ortegal, and went northward; it may have interacted with Ulla, which consistently moved southward between days 150 and 180. Figure 15 displays the trajectories, relative to the meddy center, of all other ARCANÉ float trajectories that came within a 150-km distance from the meddy center, or that started in the meddy before leaving it. Several trajectories include loops, but no persistent vortex is evidenced. Three floats complete one or two cyclonic loops in the vicinity of Ulla in the 400–600 m layer, but those loops are located south of the meddy center latitude. In the 1000–1500 m layer no persistent cyclonic looping appears.

c. Ellipticity

Figures 2 and 5 provide evidence that Meddy Ulla was significantly elliptic in mid-April and mid-August 1997, and Fig. 9d shows that a significant deviation from circular symmetry existed during the whole first year. The trajectories of floats relative to the meddy center were cautiously analyzed in order to study the evolution of the meddy ellipticity. For each individual float loop, maxima and minima of the distance to the center were isolated, and for those loops with an elliptic shape, ellipticity (here defined as b/a , ratio of minor to major axes lengths) and orientation of the major axis (angle with the zonal direction) were calculated.

Ellipticity amounts to 0.77 ± 0.08 , with a quite noisy signal and no significant trends. The calculation can be biased (notably toward low values) by errors in the float positioning, by inadequate noise filtering, and by errors in the meddy center position. We note, nevertheless, that ellipticity during the BO *D'Entrecasteaux* cruise of April 1997 and NO *Thalassa* cruise of August 1997 (Figs. 2 and 5) were around 0.7 and 0.75, so that a mean value of 0.77 cannot be ruled out.

Orientation of the ellipse main axis is displayed in Fig. 16. It is also somewhat noisy, however some clear trends can be detected. During the first 60 days, the ellipse rotates clockwise at a mean rate of $1.3^\circ \text{ day}^{-1}$. Then, for about 30 days, float trajectories become nonelliptic and dominated by mode 3 (triangular loops), so that a main orientation cannot be defined. From day 90 to day 150, the meddy shape becomes elliptic again and the main axis rotates clockwise at a $\sim 3.6^\circ \text{ day}^{-1}$ rate, completing more than a half turn from nearly 90° (meridional orientation) to -90° and back to positive orientations. From day 160 to 250, the orientation is remarkably stable to on average 35° (eastnortheast–westsouthwest). Then the angle seems to increase to 60° , decrease to 0° , increase back to around 20° , and after day 360 we lack data good enough to determine it. While the signal is admittedly noisy, we note that the orientations found after day 0 ($\sim 60^\circ$) and around day 120 ($\sim 0^\circ$) correspond nicely with the hydrological observations during *D'Entrecasteaux* and *Thalassa* cruises (Figs. 2 and 5).

The first theoretical studies of elliptical vortices in fluid mechanics date back to the nineteenth century, and oceanographic applications have been dealt with, notably, by Cushman-Roisin et al. (1985) and Young (1986) (see also references therein). The work that is the most relevant to the present application is perhaps that of Meacham (1992), who studied the behavior of a uniform ellipsoidal patch of PV anomaly in a stratified, rotating fluid. Meacham finds that the rate of rotation is linearly related to the PV anomaly and a function of the lengths of the principal axes of the ellipsoid. Application to Meddy Ulla, taking into consideration only the negative PV anomaly patch, with semiaxes 39 km (major horizontal), 31 km (minor horizontal), and 250 m (vertical), and the ratio of Brunt–Väisälä to Coriolis frequencies $N/f = 26$, gives an estimated clockwise ellipse rotation rate around 5° day^{-1} , slightly larger than the maximum observed rate. Many factors are not taken into account in this model, like the presence of the two positive PV anomaly lobes above and below, possible external flows and shears, and interactions with the topography, which could explain the discrepancy. Hebert et al. (1990) quote a 10°

day⁻¹ rotation rate for Meddy Sharon, also larger than the rate found for Ulla.

Comparing Fig. 16 with Figs. 12 and 13, we find that the first period of slow clockwise rotation corresponds to a generally southwestward drift. The period of mode 3 shape corresponds to the arrival upon the Charcot Seamounts, and to the northward U-turn. The period of rapid clockwise rotation of days 90–160 corresponds to the eastward meddy drift. Finally, the period of relatively stationary orientation corresponds to a period of meddy stagnation, in days 160–330. The meddy southwestward acceleration after day 330 is associated with more noise in the ellipse orientation. We do not have simple interpretations for these facts, which need further investigations.

d. Time evolution of hydrographic properties

Before the discovery of Meddy Ulla in April 1997, we lack any information. Altimetry data, notably, did not allow one to track back its small surface signal without ambiguity (Paillet et al. 1997). Its formation may have occurred next to the Iberian continental slope, in the Cape Finisterre–Cape Ortegal area (Fig. 1): according to Daniault et al. (1994) and recent ARCANE observations, the maximum salinity of the MW decreases from around 36.20 to around 36.0 psu between these two capes. Figure 14b provides an example of meddy formation in that area, and several others were observed by ARCANE floats.

Ulla was frequently sampled from April 1997 to the NO *Thalassa* cruise of August 1997, but much less afterward (Table 1). The series of salinity (which maxima are quoted in Table 1) are difficult to interpret in terms of meddy evolution, because salinity measurements with expendable probes lack precision (around 0.05), and because the latest cruises did not reach the meddy core. Thus we present in Fig. 17 the distribution of maximum in situ temperature in the 800–1200 dbar range, against radial distance from the meddy center, for four selected cruises. The first one, that of BO *D'Entrecasteaux* in April 1997, shows a relatively scattered temperature distribution, even within the meddy core ($R < 15$ km): three points present maximum temperatures below 11.45°C, while nine others are in the (11.49°, 11.53°C) range. This observation thus suggests that in April 1997, Meddy Ulla was still imperfectly mixed in the horizontal plane. In August 1997, the maximum temperature distribution was quite tight up to a 15-km radius (circles on Fig. 17), with values around 11.48 that could well result from the mixing of all components of the April 1997 meddy core. The overall temperature distribution shapes are similar for both cruises, showing that no significant transformation (meddy breakup or coalescence) occurred in between. In December 1997, only one hydrological profile was obtained by BH2 *Lapérouse*, with an XCTD. The maximum temperature of 11.44°C at 12 km from the meddy center is some 0.03°C below the August 1997 values, which may be due either to instrumental uncertainty or to dissipation of the meddy. Finally, in March 1998, a series of expendable probes were launched from BSHM *Alcyon* in the vicinity of, but not within, the meddy core. Maximum temperatures are quite scattered, and on average below those of August 1997 by typically 0.1°C, which is an evidence of a slight meddy dissipation. At the time of the *Alcyon* cruise, the meddy had started its fast southwestward drift. The dot with a temperature above 11°C more than 40 km away from the center (Fig. 17) is located to the northeast of the core and suggests that, while accelerating southwestward, the meddy lost some particles. Two other evidences of loss of mass by the meddy during its southwestward drift are provided by the trajectories of Marvor 656, cycle 9 [displayed in Paillet et al. (1999, plate 2)] and RAFOS 635 (Fig. 3f). Both floats were located within 15 km from the meddy center when they were ejected, the first one near day 370, and the second one near day 400.

Armi et al. (1989) describe how Meddy Sharon decayed for two years in the Canary Basin. They find that the core values of temperature and salinity did not decrease during the first year, and did decrease during the second year after lateral intrusions had reached the meddy center. Our observation of Meddy Ulla for one year is consistent with the first year of observation of Meddy Sharon, with a seemingly small decrease of the core properties.

e. Time evolution of the rotation frequency

Velocity measurements and float tracking in Meddy Sharon revealed that the rotation frequency of its core remained nearly constant (Armi et al. 1989; Richardson et al. 1989). As for Meddy Ulla, Fig. 18 shows the evolution of the rotation frequency (here counted positive clockwise) in the 5–8 km radius range, computed from float tracks as described in section 4. While the dispersion is large, a decreasing trend of 10%–20% in one year appears at 1200 and 1000 m, respectively. Assuming that the rotation frequency of a vortex satisfies a law:


$$\frac{\partial \omega}{\partial t} = \nu \nabla^2 \omega,$$

where ν is the friction coefficient at the vortex scale, a scaling yields ν to be in the 3–6 m² s⁻¹ range. These numbers compare well with the diffusion coefficients of 2 m² s⁻¹ found by Pingree and Le Cann (1992), based on the rate of separation of buoys trapped in a near-surface anticyclonic eddy, or of 10 m² s⁻¹ deduced by Colin de Verdière (1992) from

the salt content evolution of Meddy Sharon. This is how small friction and mixing coefficients should be in numerical models intended to keep meddies alive for a realistic duration.

6. Summary and discussion

A great number of meddies have been presented in recent literature, and a lot is known about them, but Meddies can be quite different from one another. Meddy Ulla is not “just another meddy,” for at least two reasons:

-It is the northernmost meddy that has ever been studied. The northernmost positions of meddies detected in historical data are also close to 45°N (Fig. 1 ) but those anomalies were not clearly identified as meddies at the time of the cruises, and not studied further.

-It is the first meddy ever observed to remain stationary for more than a few weeks (indeed, for many months). As a consequence, it is also the slowest meddy ever observed.

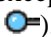
Ulla's location and hydrological properties suggest that it was born in the vicinity of the northwestern corner of Spain (Galicia), far to the north of previously known formation sites. The relatively low values of its core temperature and salinity (11.5°C and 36.17, while meddies are commonly above 12°C and 36.4) are typical of the MW vein offshore of Galicia. The fact that hydrological properties were not completely mixed within the core when it was first seen, and that on average they did not significantly evolve for a year, suggest that the meddy was young. As a likely consequence of the MW vein getting diffused and losing intensity northward along the west Iberian slope (Danialt et al. 1994), Ulla is not a very strong meddy: its maximum azimuthal velocities of 15–20 cm s⁻¹ and its Rossby number ($Ro = -0.3$, $R\Omega = 0.24$) are in the low range of previously studied Meddies (Prater and Sandford 1994; Bower et al. 1997). Nevertheless, its salinity anomaly of 0.5 relative to the neighboring environment, and the azimuthal volume transport of around 10 Sv associated with it, are quite significant.

Perhaps the most puzzling phenomenon is the near-stationarity of Ulla for 11 months. An influence of the deep Charcot Seamounts is likely, even though earlier studies (Richardson et al. 1989, 2000; Richardson and Tychensky 1998) showed many interactions between Meddies and seamounts, which resulted either in meddy destruction or track deviation, but never in long-term blocking. Interaction with the general circulation or with a neighboring cyclone, processes commonly advocated to account for anomalies in meddy tracks, could not be evidenced and seem unlikely to have forced an 11-month stagnation. Finally, a process capable of blocking the meddy could be evidenced with our data: it is the recurrent passage of other Meddies to the south of Ulla. If this is the main explanation, then Ulla's behavior must be considered as an exception to the general northern meddy behavior.

Several properties of Ulla are classical for Meddies: its vertical asymmetry, with a stronger signature near the surface than down to 2000-m depth; the smooth appearance of hydrological profiles within the core, while outside of the core the signature of mixing processes is obvious; the near solid-body rotation of its core (once ellipticity effects are filtered out); the radius of dynamical influence, much wider than the thermohaline radius.

Some other results of this study are quite original, either because Ulla was different from other meddies or because the present dataset allows investigation of properties that earlier studies could hardly deal with: Meddy Ulla was and remained significantly elliptic for most of the observation period. The evolution of the main axis orientation could be investigated using float tracks, and a noisy but significant signal stands out, with periods of slow clockwise rotation and periods of stagnation. A widening of the radial dynamical structure with decreasing depth was also observed in August 1997. This may be a consequence of the baroclinic adjustment of the upper layer over a relatively long period of time, the meddy being quite stationary at that time. The structure aligned itself with a patch of relatively fresh LSW, also bearing a negative density anomaly, between June and August 1997. Finally the radial distribution of azimuthal velocity was so variable outside of the central core, that attempts to fit it with a well-defined mathematical function seem useless.

These analyses show how Meddy Ulla was different from “simple” meddy models: It was not axisymmetric, not vertically symmetric, it did not have a uniform scale of radial velocity decrease and had a quite variable remote signature. It interacted with many other eddies, at different levels. A dedicated model study is needed to better understand why Ulla did not drift southwestward, but the complexity of the meddy shape and of the dynamical background will not make it an easy task.

A general question when considering the track of a northern Meddy like Ulla is whether those Meddies may contribute to the northward spreading of Mediterranean Water, advocated by Reid (1979) to feed the Nordic seas. McCartney and Mauritzen (2001, submitted to Progress in Oceanography) reject the hypothesis of a direct MW flow to such northern latitudes, but acknowledge that MW is a component of the water mass, carried by the North Atlantic Current, that flows into the Nordic Seas. If northern Meddies were to suffer significant erosion near 45°N, they would greatly contribute to the offshore salt diffusion, and a further northeastward advection within the North Atlantic Current could transport the salt poleward. Here Meddy Ulla's northerly position seems to be an exception; however, several other Meddies were detected in historical data, more to the west, between 44° and 45°N (Fig. 1 ) . The salt flux due to northern Meddies is currently

Acknowledgments

We are grateful to Rodolphe Rousselet for his help with the hydrological data processing and to Loic Gourmelen and Luis Lampert for the preprocessing of floats and Surdrift buoys tracks. Historical meddy properties were supplied courtesy of Philip Richardson. The ARCANE program is supported by SHOM and IFREMER.

REFERENCES

- Ambar I., and M. R. Howe, 1979: Observations of the Mediterranean Outflow. II: The deep circulation in the vicinity of the Gulf of Cadiz. *Deep-Sea Res. I*, **26A**, 555–568. [Find this article online](#)
- Arhan M., A. Colin de Verdière, and L. Mémyer, 1994: The eastern boundary of the subtropical North Atlantic. *J. Phys. Oceanogr*, **24**, 1295–1316. [Find this article online](#)
- Armi L., and W. Zenk, 1984: Large lenses of highly saline Mediterranean Water. *J. Phys. Oceanogr*, **14**, 1560–1576. [Find this article online](#)
- Armi L., D. Hebert, N. Oakey, J. F. Price, P. L. Richardson, H. T. Rossby, and B. Ruddick, 1989: Two years in the life of a Mediterranean salt lens. *J. Phys. Oceanogr*, **19**, 354–370. [Find this article online](#)
- Bower A. S., L. Armi, and I. Ambar, 1995: Direct evidence of meddy formation off the southwestern coast of Portugal. *Deep-Sea Res. I*, **42**, 1621–1630. [Find this article online](#)
- Bower A. S., L. Armi, and I. Ambar, 1997: Lagrangian observations of meddy formation during a Mediterranean undercurrent seeding experiment. *J. Phys. Oceanogr*, **27**, 2545–2574. [Find this article online](#)
- Chérubin L., X. J. Carton, and D. Dritschel, 1996: Vortex expulsion by a zonal coastal jet on a transverse canyon. *Proc. Second Int. Workshop on Vortex Flows*, Vol. 1, Paris, France, ESAIM, SMAI, 481–501.
- Chérubin L., X. J. Carton, J. Paillet, Y. Morel, and A. Serpette, 2000: Instability of the Mediterranean Water undercurrents southwest of Portugal: Effects of baroclinicity and topography. *Oceanol. Acta*, **23**, 551–573. [Find this article online](#)
- Colin de Verdière A., 1992: On the southward motion of Mediterranean salt lenses. *J. Phys. Oceanogr*, **22**, 413–420. [Find this article online](#)
- Cushman-Roisin B., W. H. Heil, and D. Nof, 1985: Oscillations and rotations of elliptical warm core rings. *J. Geophys. Res*, **90**, 11756–11764, (C6),. [Find this article online](#)
- Daniault N., J. P. Mazé, and M. Arhan, 1994: Circulation and mixing of Mediterranean Water west of the Iberian Peninsula. *Deep-Sea Res*, **41**, 1685–1714. [Find this article online](#)
- D'Asaro E. A., 1988: Generation of submesoscale vortices: A new mechanism. *J. Geophys. Res*, **93**, 6685–6693. [Find this article online](#)
- Fischer J., and M. Visbeck, 1993: Deep velocity profiling with self-contained ADCPs. *J. Atmos. Oceanic Technol*, **10**, 764–773. [Find this article online](#)
- Gould W. J., 1983: The Northeast Atlantic Ocean. *Eddies in Marine Science*, A. R. Robinson, Ed., Springer Verlag, 145–157.
- Hebert D., N. Oakey, and B. Ruddick, 1990: Evolution of a Mediterranean salt lens: Scalar properties. *J. Phys. Oceanogr*, **20**, 1468–1483. [Find this article online](#)
- Hinrichsen H.-H., M. Rhein, R. H. Käse, and W. Zenk, 1993: The Mediterranean Water tongue and its chlorofluoromethane signal in the Iberian Basin in early summer 1989. *J. Geophys. Res*, **98**, 8405–8412, (C5),. [Find this article online](#)
- Hogg N. G., and H. M. Stommel, 1985: The Heton—An elementary interaction between discrete baroclinic geostrophic vortices, and implications concerning the eddy heat flow. *Proc. Roy. Soc. London*, **397A**, 1–20.
- Jungclaus J. H., 1999: A three-dimensional simulation of the formation of anticyclonic lenses (Meddies) by the instability of an intermediate depth boundary current. *J. Phys. Oceanogr*, **29**, 1579–1598. [Find this article online](#)
- Käse R. H., and W. Zenk, 1987: Reconstructed Mediterranean salt lens trajectories. *J. Phys. Oceanogr*, **17**, 158–163. [Find this article online](#)

- Käse R. H., and W. Zenk, 1996: Structure of the Mediterranean Water and meddy characteristics in the northeastern Atlantic. *The Warmwatersphere of the North Atlantic Ocean*, E. B. Krauss, Ed., Gebrüder Borntraeger, 365–395.
- Käse R. H., A. Beckmann, and H.-H. Hinrichsen, 1989: Observational evidence of salt lens formation in the Iberian Basin. *J. Geophys. Res.*, **94**, 4905–4912, (C4),. [Find this article online](#)
- Le Cann B., K. Speer, A. Serpette, J. Paillet, and T. Reynaud, 1999:: Lagrangian observations in the intergyre northeast Atlantic during the ARCANE and EUROFLOAT projects: Early results. *WOCE Newsl.*, **34**, 25–27. [Find this article online](#)
- Madelain F., 1970: Influence de la topographie de fond sur l'écoulement Méditerranéen entre le Déroit de Gibraltar et le Cap Saint Vincent. *Cah. Oceanogr.*, **22**, 43–61.
- McCartney M. S., and C. Mauritzen, 2001: On the origin of the warm inflow into the Nordic seas. *Progress in Oceanography*, Pergamon Press, in press.
- McWilliams J. C., 1985: Submesoscale, coherent vortices in the ocean. *Rev. Geophys.*, **23**, 165–182. [Find this article online](#)
- McWilliams J. C., and G. R. Flierl, 1979: On the evolution of isolated, nonlinear vortices. *J. Phys. Oceanogr.*, **9**, 1155–1182. [Find this article online](#)
- McWilliams J. C., and P. R. Gent, 1986: The evolution of submesoscale, coherent vortices on the β -plane. *Geophys. Astrophys. Fluid Dyn.*, **35**, 235–255. [Find this article online](#)
- Meacham S. P., 1992: Quasigeostrophic, ellipsoidal vortices in a stratified fluid. *Dyn. Atmos. Oceans*, **16**, 189–223. [Find this article online](#)
- Morel Y., and J. C. McWilliams, 1997: Evolution of isolated interior vortices in the ocean. *J. Phys. Oceanogr.*, **27**, 727–748. [Find this article online](#)
- Paillet J., and H. Mercier, 1997: An inverse model of the eastern North Atlantic general circulation and thermocline ventilation. *Deep-Sea Res.*, **44**, 1293–1328. [Find this article online](#)
- Paillet J., B. Le Cann, K. Speer, and A. Serpette, 1997: Real-time observation of oceanic mesoscale structures during the ARCANE program. *Proc. Int. Symp. on Monitoring the Oceans in the 2000s: An Integrated Approach*, Biarritz, France, CNES, 3 pp. [Available from the authors.]
- Paillet J., B. Le Cann, A. Serpette, Y. Morel, and X. Carton, 1999: Real-time tracking of a Galician meddy. *Geophys. Res. Lett.*, **26**, 1877–1880. [Find this article online](#)
- Pichevin T., and D. Nof, 1996: The eddy cannon. *Deep-Sea Res. I*, **43**, 1475–1507. [Find this article online](#)
- Pingree R. D., and B. Le Cann, 1992: Anticyclonic eddy X91 in the southern Bay of Biscay, May 1991 to February 1992. *J. Geophys. Res.*, **97**, 14353–14367, (C9),. [Find this article online](#)
- Pingree R. D., and B. Le Cann, 1993a: Structure of a meddy (Bobby 92) southeast of the Azores. *Deep-Sea Res. I*, **40**, 2077–2103. [Find this article online](#)
- Pingree R. D., and B. Le Cann, 1993b: A shallow meddy (a SMEDDY) from the secondary Mediterranean salinity maximum. *J. Geophys. Res.*, **98**, 20169–20185. [Find this article online](#)
- Prater M. D., and T. B. Sanford, 1994: A meddy off Cape St. Vincent. Part I: Description. *J. Phys. Oceanogr.*, **24**, 1572–1586. [Find this article online](#)
- Reid J. L., 1979: On the contribution of the Mediterranean Sea outflow to the Norwegian–Greenland Sea. *Deep-Sea Res.*, **26**, 1199–1223. [Find this article online](#)
- Richardson P. L., and A. Tychensky, 1998: Meddy trajectories in the Canary Basin measured during the SEMAPHORE experiment, 1993–1995. *J. Geophys. Res.*, **103**, 25029–25045, (C11),. [Find this article online](#)
- Richardson P. L., D. Walsh, L. Armi, M. Schröder, and J. F. Price, 1989: Tracking three meddies with SOFAR floats. *J. Phys. Oceanogr.*, **19**, 371–383. [Find this article online](#)
- Richardson P. L., M. S. McCartney, and C. Maillard, 1991: A search for meddies in historical data. *Dyn. Atmos. Oceans*, **15**, 241–265. [Find this article online](#)
- Richardson P. L., A. S. Bower, and W. Zenk, 2000: A census of meddies tracked by floats. *Progress in Oceanography*, Vol. 45, Pergamon Press, 209–250.

Schultz Tokos K., and T. Rossby, 1991: Kinematics and dynamic of a Mediterranean salt lens. *J. Phys. Oceanogr*, **21**, 879–892. [Find this article online](#)

Schultz Tokos K., H. H. Hinrichsen, and W. Zenk, 1994: Merging and migration of two meddies. *J. Phys. Oceanogr*, **24**, 2129–2141. [Find this article online](#)

Serra N., S. Sadoux, I. Ambar, and D. Renouard, 2002: Observations and laboratory modeling of meddy generation at Cape St. Vincent. *J. Phys. Oceanogr*, **32**, 3–25. [Find this article online](#)

Shapiro G. I., and S. L. Meschanov, 1996: Spreading pattern and mesoscale structure of Mediterranean Outflow in the Iberain Basin estimated from historical data. *J. Mar. Syst*, **7**, 337–348. [Find this article online](#)

Stammer D., H.-H. Hinrichsen, and R. H. Käse, 1991: Can Meddies be detected by satellite altimetry? *J. Geophys. Res*, **96**, 7005–7014, (C4),. [Find this article online](#)

Thierry V., and Y. Morel, 1999: Influence of a strong bottom slope on the evolution of a surface-intensified vortex. *J. Phys. Oceanogr*, **29**, 911–924. [Find this article online](#)

Tychensky A., and X. Carton, 1998: Hydrological and dynamical characterization of meddies in the Azores region: A paradigm for baroclinic vortex dynamics. *J. Geophys. Res*, **103**, 25061–25079, (C11),. [Find this article online](#)

Vandermeirsch F., Y. Morel, and G. Sutyryn, 2001: The net advective effect of a vertically sheared current on a coherent vortex. *J. Phys. Oceanogr*, **31**, 2210–2225. [Find this article online](#)

van Geffen J. H. G. M., and P. A. Davies, 2000: A monopolar vortex encounters an isolated feature on a β -plane. *Dyn. Atmos. Ocean*, **32**, 1–26. [Find this article online](#)

Young W. R., 1986: Elliptical vortices in shallow water. *J. Fluid Mech*, **171**, 101–119. [Find this article online](#)

Zenk W., 1975: On the Mediterranean Outflow west of Gibraltar. *Meteor. Forschungsgeb. A*, **16**, 15–22. [Find this article online](#)

Tables

TABLE 1. Summary of all measurements and float deployments in Meddy Ulla. In the “floats/buoys” column, “S” stands for Surdrift, “R” for RAFOS, and “M” for Marvor. When ellipticity could be resolved by the measurements, major and minor axes lengths are indicated

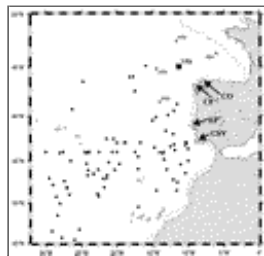
Date	Ship	Measurement	Float/Buoy depth, depth	Min. distance from center	Major distance	ζ_{max}
11-12 Apr 97	BDP Entomoceros	SUR, NCTD, CTD-LADCP	545, 1100 m 505, 1200 m 803, 1420 m	-3 km	45 km (maj) 40 km (min)	26.7 CTD
11-13 May 97	BDM Albat	SUR, NCTD	545, 1100 m 803, 1420 m	-4 km	-50 km	36.5 CTD
11-14 Jun 97	BDI Lapr cruise	SUR, NCTD, CTD-LADCP	545, 1100 m 803, 1420 m	-4 km	-50 km	26.7 CTD
20-21 Jun 97	BDP Entomoceros	SUR, NCTD	530, 130 m	-4 km	—	36.5 CTD
11-16 Aug 97	BDI Thalita	CTD-LADCP	545, 1100 m 803, 1420 m 1012, 1500 m 1012, 1500 m	-4 km	40 km (maj) 40 km (min)	37.7 CTD
1 Dec 97	BDI Lapr cruise	sur, NCTD	530, 130 m	-10 km	—	36.5 CTD
20 Jun 98	BDM Albat	SUR, NCTD	545, 1100 m	-10 km	30 km	36.5 CTD
21 Apr 98	BDP Entomoceros	CTD, SUR, NCTD	530, 130 m	-20 km	—	36.5 CTD

Click on thumbnail for full-sized image.

TABLE 2. Information on floats which looped in Meddy Ulla. “S” stands for Surdrift, “R” for Rafos and “M” for Marvor. Floats annotated with an * were not originally released in the meddy

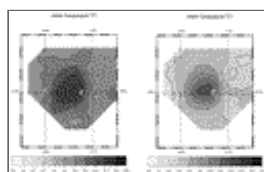
Float type and number	Anchor depth (m) or pressure (dbar)	Start date/ period (day)	Time of release	Period (days)	Number of loops	Mean distance from center (km)	Mean radius (km)
11-524	1100 m	2 months	15 Aug 1997	15097-15097	2	70	11.0
1-134	1200 m	2 months	15 Aug 1997	15097-15097	23	4.3	3.9
1-134*	1100 m	1 year	15 Aug 1997	15097-15098	68	2.7	2.7
1-134	1200 m	1 year	15 Aug 1997	15097-15098	68	4.2	3.1
1-134	1000 m	2 months	15 Aug 1997	15097-15100	16	6.0	5.0
1-134	1200 m	2 months	15 Aug 1997	15097-15100	16	6.0	5.0
1-134	1000 m	2 months	15 Aug 1997	15097-15100	16	6.0	5.0
1-134	1200 m	2 months	15 Aug 1997	15097-15100	16	6.0	5.0
1-134	1000 m	2 months	15 Aug 1997	15097-15100	16	6.0	5.0
1-134	1200 m	2 months	15 Aug 1997	15097-15100	16	6.0	5.0
1-134	1000 m	2 months	15 Aug 1997	15097-15100	16	6.0	5.0
1-134	1200 m	2 months	15 Aug 1997	15097-15100	16	6.0	5.0
1-134	1000 m	2 months	15 Aug 1997	15097-15100	16	6.0	5.0
1-134	1200 m	2 months	15 Aug 1997	15097-15100	16	6.0	5.0
1-134	1000 m	2 months	15 Aug 1997	15097-15100	16	6.0	5.0
1-134	1200 m	2 months	15 Aug 1997	15097-15100	16	6.0	5.0
1-134	1000 m	2 months	15 Aug 1997	15097-15100	16	6.0	5.0
1-134	1200 m	2 months	15 Aug 1997	15097-15100	16	6.0	5.0
1-134	1000 m	2 months	15 Aug 1997	15097-15100	16	6.0	5.0
1-134	1200 m	2 months	15 Aug 1997	15097-15100	16	6.0	5.0
1-134	1000 m	2 months	15 Aug 1997	15097-15100	16	6.0	5.0
1-134	1200 m	2 months	15 Aug 1997	15097-15100	16	6.0	5.0
1-134	1000 m	2 months	15 Aug 1997	15097-15100	16	6.0	5.0
1-134	1200 m	2 months	15 Aug 1997	15097-15100	16	6.0	5.0
1-134	1000 m	2 months	15 Aug 1997	15097-15100	16	6.0	5.0
1-134	1200 m	2 months	15 Aug 1997	15097-15100	16	6.0	5.0
1-134	1000 m	2 months	15 Aug 1997	15097-15100	16	6.0	5.0
1-134	1200 m	2 months	15 Aug 1997	15097-15100	16	6.0	5.0
1-134	1000 m	2 months	15 Aug 1997	15097-15100	16	6.0	5.0
1-134	1200 m	2 months	15 Aug 1997	15097-15100	16	6.0	5.0
1-134	1000 m	2 months	15 Aug 1997	15097-15100	16	6.0	5.0
1-134	1200 m	2 months	15 Aug 1997	15097-15100	16	6.0	5.0
1-134	1000 m	2 months	15 Aug 1997	15097-15100	16	6.0	5.0
1-134	1200 m	2 months	15 Aug 1997	15097-15100	16	6.0	5.0
1-134	1000 m	2 months	15 Aug 1997	15097-15100	16	6.0	5.0
1-134	1200 m	2 months	15 Aug 1997	15097-15100	16	6.0	5.0
1-134	1000 m	2 months	15 Aug 1997	15097-15100	16	6.0	5.0
1-134	1200 m	2 months	15 Aug 1997	15097-15100	16	6.0	5.0
1-134	1000 m	2 months	15 Aug 1997	15097-15100	16	6.0	5.0
1-134	1200 m	2 months	15 Aug 1997	15097-15100	16	6.0	5.0
1-134	1000 m	2 months	15 Aug 1997	15097-15100	16	6.0	5.0
1-134	1200 m	2 months	15 Aug 1997	15097-15100	16	6.0	5.0
1-134	1000 m	2 months	15 Aug 1997	15097-15100	16	6.0	5.0
1-134	1200 m	2 months	15 Aug 1997	15097-15100	16	6.0	5.0
1-134	1000 m	2 months	15 Aug 1997	15097-15100	16	6.0	5.0
1-134	1200 m	2 months	15 Aug 1997	15097-15100	16	6.0	5.0
1-134	1000 m	2 months	15 Aug 1997	15097-15100	16	6.0	5.0
1-134	1200 m	2 months	15 Aug 1997	15097-15100	16	6.0	5.0
1-134	1000 m	2 months	15 Aug 1997	15097-15100	16	6.0	5.0
1-134	1200 m	2 months	15 Aug 1997	15097-15100	16	6.0	5.0
1-134	1000 m	2 months	15 Aug 1997	15097-15100	16	6.0	5.0
1-134	1200 m	2 months	15 Aug 1997	15097-15100	16	6.0	5.0
1-134	1000 m	2 months	15 Aug 1997	15097-15100	16	6.0	5.0
1-134	1200 m	2 months	15 Aug 1997	15097-15100	16	6.0	5.0
1-134	1000 m	2 months	15 Aug 1997	15097-15100	16	6.0	5.0
1-134	1200 m	2 months	15 Aug 1997	15097-15100	16	6.0	5.0
1-134	1000 m	2 months	15 Aug 1997	15097-15100	16	6.0	5.0
1-134	1200 m	2 months	15 Aug 1997	15097-15100	16	6.0	5.0
1-134	1000 m	2 months	15 Aug 1997	15097-15100	16	6.0	5.0
1-134	1200 m	2 months	15 Aug 1997	15097-15100	16	6.0	5.0
1-134	1000 m	2 months	15 Aug 1997	15097-15100	16	6.0	5.0
1-134	1200 m	2 months	15 Aug 1997	15097-15100	16	6.0	5.0
1-134	1000 m	2 months	15 Aug 1997	15097-15100	16	6.0	5.0
1-134	1200 m	2 months	15 Aug 1997	15097-15100	16	6.0	5.0
1-134	1000 m	2 months	15 Aug 1997	15097-15100	16	6.0	5.0
1-134	1200 m	2 months	15 Aug 1997	15097-15100	16	6.0	5.0
1-134	1000 m	2 months	15 Aug 1997	15097-15100	16	6.0	5.0
1-134	1200 m	2 months	15 Aug 1997	15097-15100	16	6.0	5.0
1-134	1000 m	2 months	15 Aug 1997	15097-15100	16	6.0	5.0
1-134	1200 m	2 months	15 Aug 1997	15097-15100	16	6.0	5.0
1-134	1000 m	2 months	15 Aug 1997	15097-15100	16	6.0	5.0
1-134	1200 m	2 months	15 Aug 1997	15097-15100	16	6.0	5.0
1-134	1000 m	2 months	15 Aug 1997	15097-15100	16	6.0	5.0
1-134	1200 m	2 months	15 Aug 1997	15097-15100	16	6.0	5.0
1-134	1000 m	2 months	15 Aug 1997	15097-15100	16	6.0	5.0
1-134	1200 m	2 months	15 Aug 1997	15097-15100	16	6.0	5.0
1-134	1000 m	2 months	15 Aug 1997	15097-15100	16	6.0	5.0
1-134	1200 m	2 months	15 Aug 1997	15097-15100	16	6.0	5.0
1-134	1000 m	2 months	15 Aug 1997	15097-15100	16	6.0	5.0
1-134	1200 m	2 months	15 Aug 1997	15097-15100	16	6.0	5.0
1-134	1000 m	2 months	15 Aug 1997	15097-15100	16	6.0	5.0
1-134	1200 m	2 months	15 Aug 1997	15097-15100	16	6.0	5.0
1-134	1000 m	2 months	15 Aug 1997	15097-15100	16	6.0	5.0
1-134	1200 m	2 months	15 Aug 1997	15097-15100	16	6.0	5.0
1-134	1000 m	2 months	15 Aug 1997	15097-15100	16	6.0	5.0
1-134	1200 m	2 months	15 Aug 1997	15097-15100	16	6.0	5.0
1-134	1000 m	2 months	15 Aug 1997	15097-15100	16	6.0	5.0
1-134	1200 m	2 months	15 Aug 1997	15097-15100	16	6.0	5.0
1-134	1000 m	2 months	15 Aug 1997	15097-15100	16	6.0	5.0
1-134	1200 m	2 months	15 Aug 1997	15097-15100	16	6.0	5.0
1-134	1000 m	2 months	15 Aug 1997	15097-15100	16	6.0	5.0
1-134	1200 m	2 months	15 Aug 1997	15097-15100	16	6.0	5.0
1-134	1000 m	2 months	15 Aug 1997	15097-15100	16	6.0	5.0
1-134	1200 m	2 months	15 Aug 1997	15097-15100	16	6.0	5.0
1-134	1000 m	2 months	15 Aug 1997	15097-15100	16	6.0	5.0
1-134	1200 m	2 months	15 Aug 1997	15097-15100	16	6.0	5.0
1-134	1000 m	2 months	15 Aug 1997	15097-15100	16	6.0	5.0
1-134	1200 m	2 months	15 Aug 1997	15097-15100	16	6.0	5.0
1-134	1000 m	2 months	15 Aug 1997	15097-15100	16	6.0	5.0
1-134	1200 m	2 months	15 Aug 1997	15097-15100	16	6.0	5.0
1-134	1000 m	2 months	15 Aug 1997	15097-15100	16	6.0	5.0
1-134	1200 m	2 months	15 Aug 1997	15097-15100	16	6.0	5.0
1-134	1000 m	2 months	15 Aug 1997	15097-1			

Figures



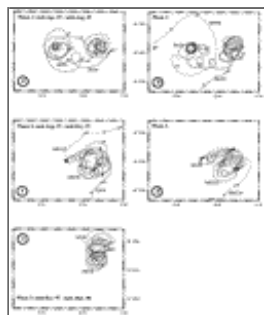
Click on thumbnail for full-sized image.

FIG. 1. Geographic context. Meddies detected from historical data by [Richardson et al. \(1991\)](#) and [Shapiro and Meschanov \(1996\)](#) are displayed as circles, and Meddy Ulla, at the location of discovery, as a square. Crosses represent the acoustic sources used to track Marvor and RAFOS floats; EP: colons Estramadura Promontory, CSV: Cape St. Vincent, CF: Cape Finisterre, and CO: Cape Ortegal. Bathymetric contour 200 m is shown



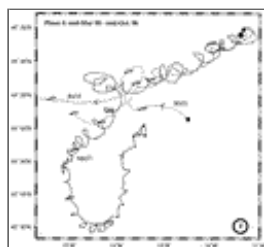
Click on thumbnail for full-sized image.

FIG. 2. Horizontal fields of in situ temperature at 1000 and 1200 m, objectively mapped from BO *D'Entrecasteaux* measurements in Apr 1997. Points from the second phase of the cruise (see [Table 1](#)) were shifted geographically to correct for the meddy displacement between the two phases, so that the fields represent the situation of 13–15 Apr 1997. Dots represent XBTs/XCTDs, stars represent CTD stations

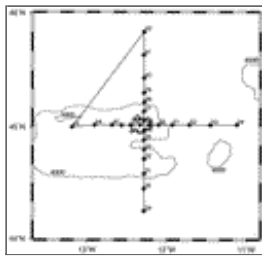


Click on thumbnail for full-sized image.

FIG. 3. Float and buoy trajectories within, or around, the meddy. (a) S834 drogued at 1100 m (dash–dotted) and S836 drogued at 1200 m (solid) during phase 1. (b) R634 around 1200 dbar (solid), R639 around 1450 dbar (dash–dotted), and M404 around 1000 dbar (dotted) during phase 1. (c) M656 around 1000 dbar (solid), M8122 around 2000 dbar (dotted), and S494 drogued at 150m (dash–dotted) during phase 2. (d) R634 around 1200 dbar (solid), M8123 around 1500 dbar (dash–dotted), and M8124 around 450 dbar (dotted) during phase 2. (e) M656 around 1000 dbar (solid) and S509 drogued at 1000 m (dotted) during phase 3. (f) M657 around 1000 dbar (solid), R635 around 1200 dbar (dash–dotted), and R651 around 1150 dbar (dotted) during phase 4. Elapsed time in days since 15 Apr 1997 is marked every 30 days on each trajectory. Black circles mark the starting point of float trajectories (or Marvor cycles at depth), while black squares indicate the beginning of bits of longer trajectories

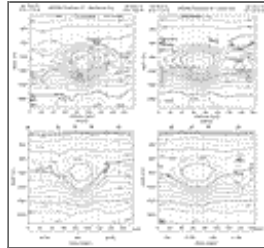


Click on thumbnail for full-sized image.



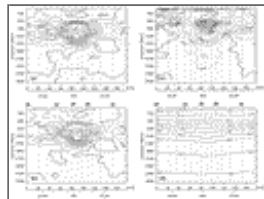
[Click on thumbnail for full-sized image.](#)

FIG. 4. Stations of NO *Thalassa* cruise on the meddy in Aug 1997. Also shown are the trajectory of RAFOS 634 near 1200 dbar, at the same time (white diamonds every 8 h, and thick line), and bathymetric contours 3000 and 4000 m



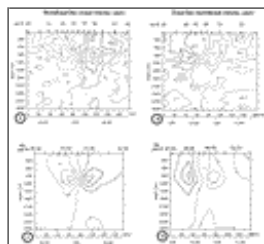
[Click on thumbnail for full-sized image.](#)

FIG. 5. Sections of salinity (upper) and potential temperature (lower) along the meridional (left) and zonal (right) *Thalassa* 97 lines. Solid line spacing is 1°C and 0.1 psu. Isocontours 3.5°, 4.5°, 9.5°, 10.5°, and 11.5°C, 34.95 and 36.15 psu are marked as dashed lines. Some station numbers are shown on top of lower figures. Latitude–longitude scale is added at the bottom of lower figures



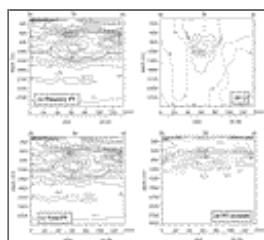
[Click on thumbnail for full-sized image.](#)

FIG. 6. Properties along the *Thalassa* 97 meridional line: (a) salinity anomaly (contour interval: 0.1); (b) temperature anomaly (c.i.: 0.5°C); (c) potential density σ_1 anomaly (c.i.: 0.01 kg m⁻³); (d) potential density σ_1 (c.i.: 0.1 kg m⁻³)



[Click on thumbnail for full-sized image.](#)

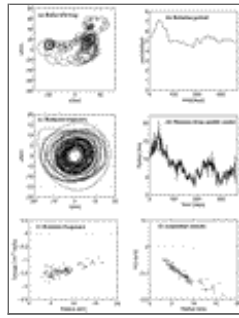
FIG. 7. Velocity components (cm s⁻¹) across the *Thalassa* 97 sections. (a) and (b) LADCP velocity across the meridional and zonal lines. (c) and (d) Cyclo-geostrophic velocity across the meridional and zonal lines



[Click on thumbnail for full-sized image.](#)

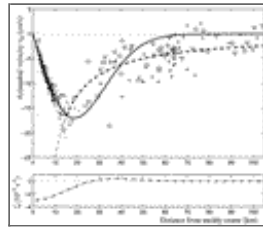
FIG. 8. Components of Ertel's potential vorticity along the *Thalassa* 97 meridional line: (a) planetary vorticity and (b) normalized relative vorticity ω/f . (c) Total PV, (d) Isopycnic anomaly of total PV, relative to the outermost stations of the line; the zero

contour is omitted for better legibility. Units in (a), (c) and (d) are $10^{-11} \text{ m}^{-1} \text{ s}^{-1}$



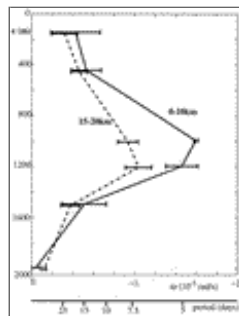
[Click on thumbnail for full-sized image.](#)

FIG. 9. Steps in the processing of RAFOS R634 trajectory: (a) trajectory of the float (solid) and of the meddy center (dotted) relative to 45°N , 12°W ; (b) evolution of the rotation period of the float; (c) trajectory relative to the meddy center; (d) evolution of the distance between float and meddy center; (e) rotation frequency against distance float–meddy center; (f) azimuthal velocity against distance float–meddy center



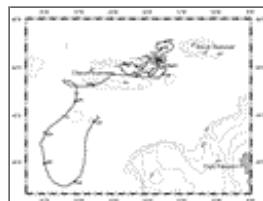
[Click on thumbnail for full-sized image.](#)

FIG. 10. Distribution of azimuthal velocity against distance from the meddy center. Dots come from Lagrangian floats R634, R635, and M656 data and are corrected for ellipticity. The “+” come from M404, triangles “ ∇ ” from R650, “x” from R 651 (uncorrected), and circles from *Thalassa 97* LADCP data (corrected). The Rankine-like fit is shown with dashed lines, and the Rayleigh fit with a solid line (see text). The vorticity associated with the Rayleigh fit is displayed with a dash–dotted line, the corresponding scale being given on the bottom of the left axis



[Click on thumbnail for full-sized image.](#)

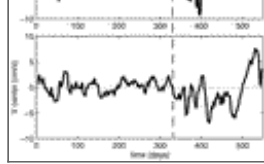
FIG. 11. Vertical distribution of rotation frequency ω , deduced at 150 m from S502 and S494, at 450 m from M8124, at 1000 m from M656 and M404, at 1200 m from R634, R635, R650, and R651, at 1500 m from R639 and M8123, and at 2000 m from M8122. The rotation frequency for radii between 0 and 10 km is shown with a solid line, and that between 15 and 20 km with a dashed line. Error bars are standard deviations



[Click on thumbnail for full-sized image.](#)

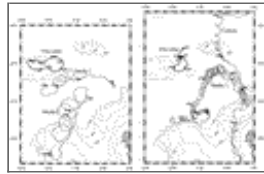
FIG. 12. Full trajectory of the meddy center, deduced from float tracks. Elapsed time in days since 15 Apr 1997 is marked every 30 days. Bathymetric contours 200, 1000, 2000, 3000, 3500, and 4000 m are shown





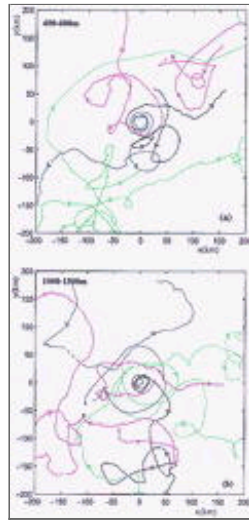
Click on thumbnail for full-sized image.

FIG. 13. Velocity components of the meddy center. (top) Zonal velocity; (bottom) meridional velocity. The dashed line marks day 330, when the meddy reaches its northernmost position and starts accelerating southwestward



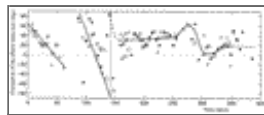
Click on thumbnail for full-sized image.

FIG. 14. Trajectories of four vortices together with portions of Ulla's center displacement. (left) Both meddies are revealed by Marvor floats near 1000 dbar. The Marvor in meddy 1 was in the meddy during only one 3-month cycle. The Marvor in meddy 2 was originally released in it, and remained in it after the 3-months cycle shown. (right) The cyclone is revealed by a RAFOS near 520 dbar, and the meddy by a RAFOS near 1200 dbar. Elapsed time in days since 15 Apr 1997 is marked every 30 days



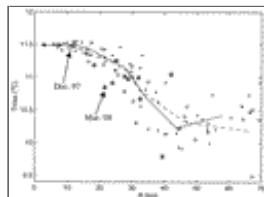
Click on thumbnail for full-sized image.

FIG. 15. Trajectories of a selection of ARCANE floats, in two depth ranges, that sampled a midrange distance (50–200 km) from the meddy core. Coordinates x and y are relative to the position of Ulla's center. (a) In the 400–600 m depth range: Marvors 8124 (blue) and 402 (red), Rafos 880 (magenta), 882 (black), 633 (cyan), and 645 (green). (b) In the 1000–1500-m depth range: Marvors 8123 (red), 404 (blue), and 406 (magenta); RAFOS 639 (black), 650 (cyan), and 651 (green). The four other trajectories that came within midrange distance of Ulla are displayed separately in [Fig. 14](#)



Click on thumbnail for full-sized image.

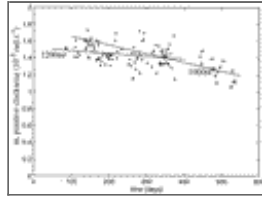
FIG. 16. Time evolution of the ellipse main axis orientation, deduced from R634 (+), R635 (*), S 834 (∇), S 836 (□), M656 (○). An empirical fit is proposed



Click on thumbnail for full-sized image.

FIG. 17. Distribution of the maximum in situ temperature in the 800–1200 m depth range, against distance from the meddy center,

for four cruises: *D'Entrecasteaux*, Apr 1997 (dots); *Thalassa*, Aug 1997 (circles); *Lapérouse*, Dec 1997 (diamond); *Alcyon*, Mar 1998 (stars). Solid and dashed lines are least squares fits by segments through Apr 1997 data and Aug 1997 data, respectively



[Click on thumbnail for full-sized image.](#)

FIG. 18. Evolution of the rotation frequency ω , in the 5–8 km radius range, deduced from floats R634 and R635 at 1200 m (dots), and M656 and M657 at 1000 m (crosses). Solid lines are least squares fits to the data at 1000 and 1200 m

Corresponding author address: Dr. Yves Morel, EPSHOM/CMO, BP 30316, Brest Cedex 29603, France. E-mail: morel@shom.fr

¹ Also named Tagus Plateau or Tejo Plateau in other works.

² Horizontal vortex scale, or half wavelength; of $\pi \times 20$ km in this area.

³ A more precise determination of that number, using floats, will give -0.3 (see [section 4c](#))

[top](#) ▲



© 2008 American Meteorological Society [Privacy Policy and Disclaimer](#)
Headquarters: 45 Beacon Street Boston, MA 02108-3693
DC Office: 1120 G Street, NW, Suite 800 Washington DC, 20005-3826
amsinfo@ametsoc.org Phone: 617-227-2425 Fax: 617-742-8718
[Allen Press, Inc.](#) assists in the online publication of *AMS* journals.